Research article

Design space exploration of an innovative tension leg platform (TLP) floating wind installation vessel

International Shipbuilding Progress
2025, Vol. 72(1) 20–50

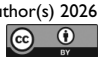

DOI: 10.1177/0020868X261435438
journals.sagepub.com/home/shp

Jesse J Flierman[1,2], Vera C Terlouw[2], André LJ Steenhuis[2] and Austin A Kana[1]

Abstract

This paper presents a design space exploration (DSE) for the development of an innovative special-purpose installation vessel for tension leg platform (TLP) floating offshore wind turbines. The concept, named "Windchanger," features an installation deck integrated with the stern design to facilitate turbine lowering and recovery. The DSE model conducts a tradeoff analysis using a parametric model of the hull and installation deck, evaluating both technical feasibility and cost-effectiveness. The model evaluates various scenarios across two demonstration operational areas: the North Sea and the U.S. East Coast. Results evaluated the principle design limitation across various TLP designs, ship concepts, installation design concepts, and operational scenarios. Findings indicate that the transport capacity measured in the number of TLPs, from 1 to 5, has a significant influence on design considerations and economic effectiveness. The overall results show that the Windchanger concept has the potential to be a competitive installation solution.

Keywords

offshore wind installation vessel design, design space exploration, TLP installation, windchanger

Received: 28 February 2025; accepted: 9 March 2026

1 Introduction

It is expected that by 2050, the contribution of offshore wind will reach 40% of the total wind production.[1] Short-term projections show that a significant number of offshore bottom-founded

[1]Department of Maritime and Transport Technology, Delft University of Technology, the Netherlands
[2]Allseas, the Netherlands

Corresponding author:
Austin A Kana, Department of Maritime and Transport Technology, Delft University of Technology, the Netherlands.
Email: a.a.kana@tudelft.nl

wind projects are planned;[2] however, in the long-term, the development of floating wind shows great promise since the majority of the world's offshore wind energy potential is located in deeper waters, where bottom-founded wind turbines are not economically viable.[3] By 2050, it is expected that floating offshore wind turbines (FOWTs) will generate approximately 15% of all offshore wind energy.[1] However, the economic viability remains a challenge for floating wind due to the high foundation costs, the uncertainty in floater design, and technology immaturity.[4] A significant step needs to be taken to reduce the levelized cost of energy, making large-scale deployment of this technology feasible. This research recognizes a great potential for the tension leg platform (TLP) floater due to the following benefits:[3]

- cost-saving due to the lower structural weight compared to other floater types,
- high stability and low motions,
- simple & light structure, designed for ease of operation and maintenance,
- wide water-depth flexibility, and
- small seabed footprint.

While installation methods for spars, barges, and semi-submersibles have been covered in both literature and practice,[5,6] an unaddressed challenge arises with TLP installation.[7] These challenges arise from the inherent instability of the pre-assembled FOWT during transport and installation, as well as the significant required downward pressure to submerge the TLP for tendon connection.[8,9] To address this challenge, this research explores an innovative installation vessel concept intended to commission fully assembled wind turbines (FAWTs) with TLP foundations. This paper explores the design space to find both a technically feasible and cost-effective solution. An exploration into the key parameters affecting both ship design and cost-effectiveness under variable conditions is performed. The feasibility of integrating ship design with TLP design will be explored along with the overall cost-effectiveness.

2 Design requirements

To start, design requirements were developed taking into account the following three key challenges.

(1) **Offshore assembly**: Current state-of-the-art FAWT assembly prioritizes single-lift installation and inshore assembly, reducing the complexity of offshore hoisting operations.
(2) **Offshore mating**: With single-lift installations, the main challenge involves the mating process of the FAWT and the foundation.
(3) **TLP installation**: The main challenge in TLP installation is submerging the structure effectively, particularly when the FAWT is pre-installed.

The primary functional requirements involve transport and installation capabilities. The concept must have the capacity to handle and store state-of-the-art, fully pre-assembled TLP FOWT(s). Transporting the FOWT fully assembled aims to mitigate the first two challenges. The state-of-the-art TLPs include three-legged designs.[10,11] Additionally, the TLP should be able to accommodate a 20 MW turbine. The only hard mission requirement is that the FOWT is transported and installed fully assembled, according to the following concept of operations:

(1) Loading and sea-fastening the fully assembled FAWT(s) in the marshaling port.

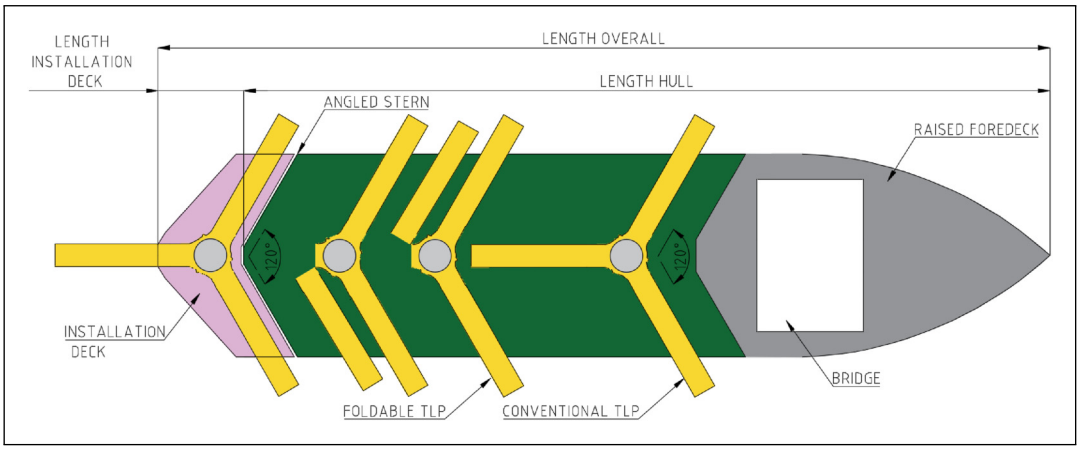

Figure 1. Deck layout of the Windchanger.

(2) Sail to the construction site of the wind farm.
(3) Upon arrival, the installation procedure starts. Depending on the transport capacity, this process might be performed repeatedly:
   (a) vessel is positioned above the pre-installed tendons using dynamic positioning (DP),
   (b) the TLP is lowered to operational draft,
   (c) the tendons are connected to the submerged TLP, and
   (d) the vessel sails away from the TLP.
(4) Finally, the vessel sets sail back to the marshaling port for the next operation.

3 Design space exploration (DSE) and parametric modeling approach

This section describes the concept generation and evaluation model used for the DSE. The proposed concept, named "Windchanger," involves a special unloading device integrated into the vessel's stern design (see Figures 1 and 2). This special unloading device is called the installation deck (ID), which is lowered by ballast water and controlled by a winch mechanism. The development of the winch mechanism was excluded from the scope of this research, but is nevertheless shown schematically in Figure 2. However, its operational principle was modeled to gain insight into the functional requirements and behavior of such a system. The winch is mechanically linked to the ID and serves solely to lower and retrieve the ID in a controlled and stable manner. Within this concept, loading is performed via skidding the FAWTs on board from the quayside. The design space is the set of all possible design solutions,[12] representing unique combinations of hull shape, ID, TLP design, and operational scenarios. For the exploration, a parametric modeling approach was employed.

3.1 Parametric model description

Figure 3 shows the parametric model's top-level modules, involving the hull generation module, the ship design module, and the economics module. The model is tailored to the Windchanger concept to examine its technical feasibility and cost-effectiveness across various scenarios. The initial

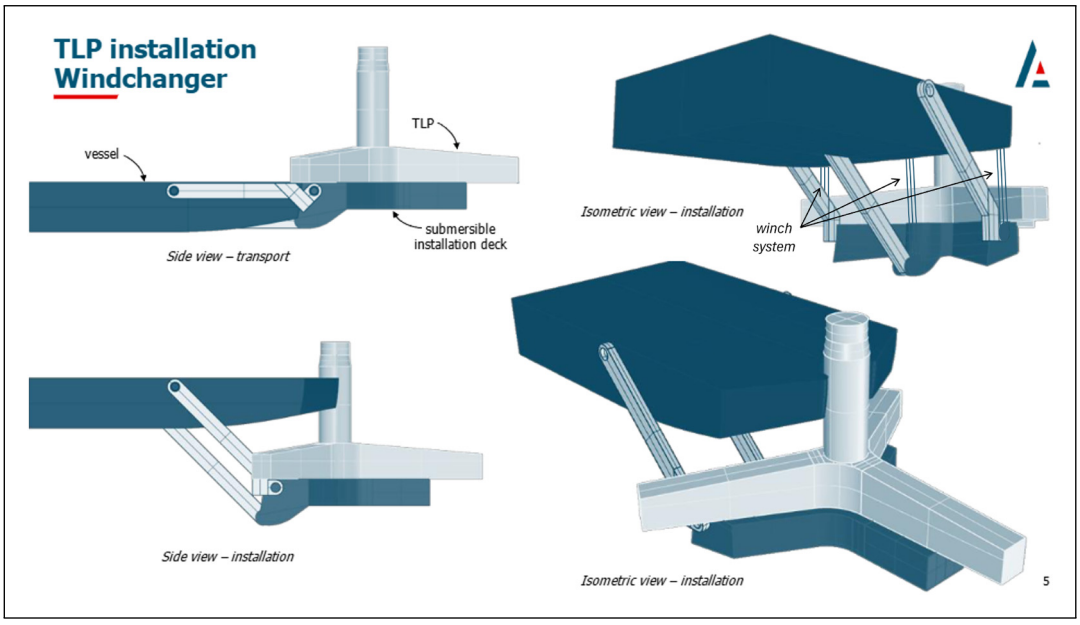

Figure 2. Proposed concept for the Windchanger installation deck.

module focuses on generating multiple hull designs and extracting their hydrostatic properties. The ship design module uses these properties to assess technical feasibility and conduct preliminary calculations necessary for the economics module.

3.2 Hull generation module

Due to the complexity of the installation operation and vessel design, the parametric model generated three-dimensional (3D) hull surfaces to ensure more detailed hydrostatic and intact stability calculations. To do this, a Python model was developed that controls Rhinoceros 3D to automate hull design and hydrostatic calculations. This module generates a unique hull surface by incorporating a range of variable ship particulars, various ID designs, and a database of parent hulls. It then calculates essential hydrostatic characteristics and hull coefficients. The output of this module serves as the input for the ship design module.

3.2.1 Variable ship particulars. The variable ship particulars have been chosen due to their expected influence on both technical feasibility and cost-effectiveness. A full factorial approach was performed to delineate the boundaries of the concept, understand its feasibility, and identify influential factors for cost-effectiveness performance. The main design parameters are varied according to Table 1. Based on these input ranges, 100,115 hull designs were generated, with an average calculation time of 7 s per hull. The depth of the cargo deck is calculated as the distance from the keel of the vessel to the top of the cargo deck. The maximum beam is restricted by the boundaries of the Holtrop and Mennen resistance approach,[13] and length overall, L_{OA}, is calculated using,

$$L_{OA} = \left(1 + \frac{\alpha_{bow}}{1 - \alpha_{bow}}\right) \cdot L_{deck} \tag{1}$$

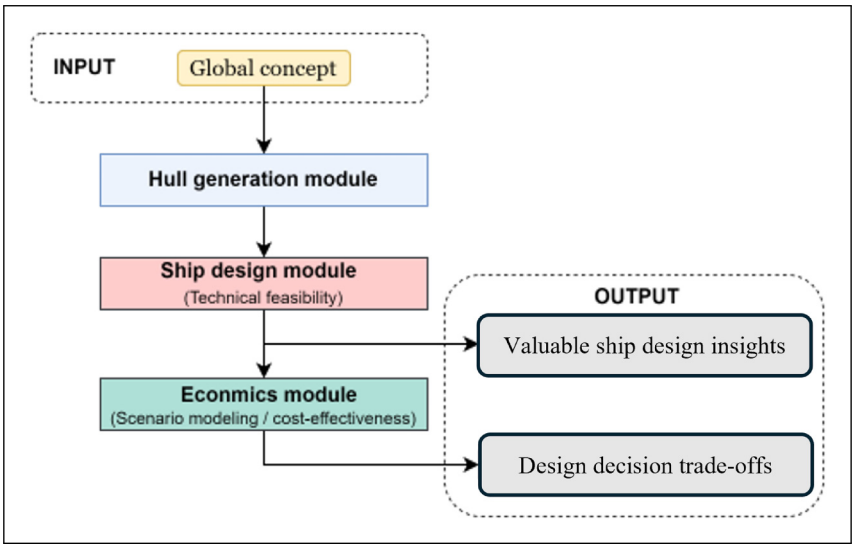

Figure 3. The top-level modules of the design exploration model.

Table 1. Input ship design particulars.

	Start	End	Step size	Unit
Length of the cargo deck (L_{deck})	30	240	15	[m]
Length ratio raised foredeck (α_{bow})	0.2	0.3	0.1	[–]
Beam	40	75	2.5	[m]
Depth of the cargo deck	12	18	1	[m]
Draft	6	12	0.5	[m]
Block coefficient	0.65	0.92	0.05	[–]

3.2.2 ID design. The design of the ID significantly influences the ship's design. During installation conditions, a substantial portion of the vessel is submerged, affecting the ship's stability and motion behavior. Three different IDs (Figure 4) ranging from full to slender were examined to assess their impact on stability, winch load, ballast water capacity, and cost-effectiveness. The depth of the ID is calculated using,

$$D_{\text{installation;deck}} = D_{\text{cargo;deck}} - C \tag{2}$$

where

- $D_{\text{installation;deck}}$ is the depth of the ID,
- $D_{\text{cargo;deck}}$ is the depth of the vessel itself, and
- C is the minimum draft of the generated ship hulls.

A fixed value of 6 m is assumed for C corresponding to the minimum draft of the generated ship hulls. A fixed deck length of 30 m, measured from the vessel's reference axis, which is centered

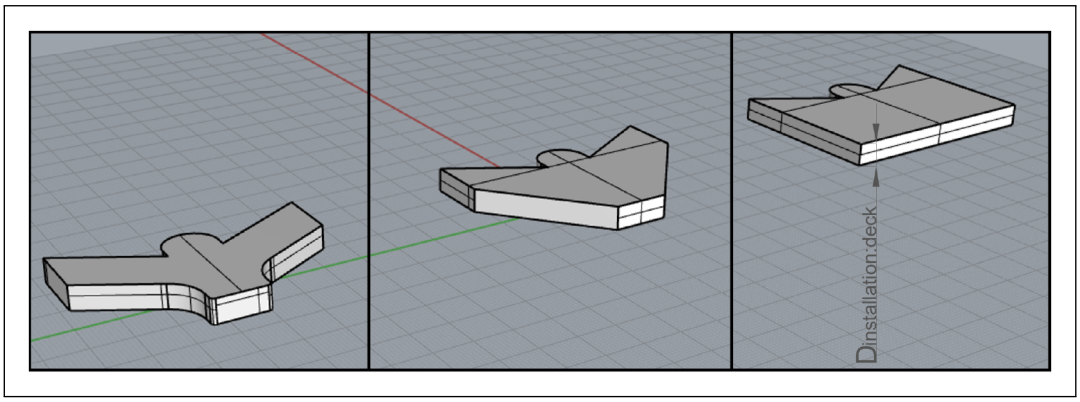

Figure 4. The different installation deck designs (slender — intermediate — full).

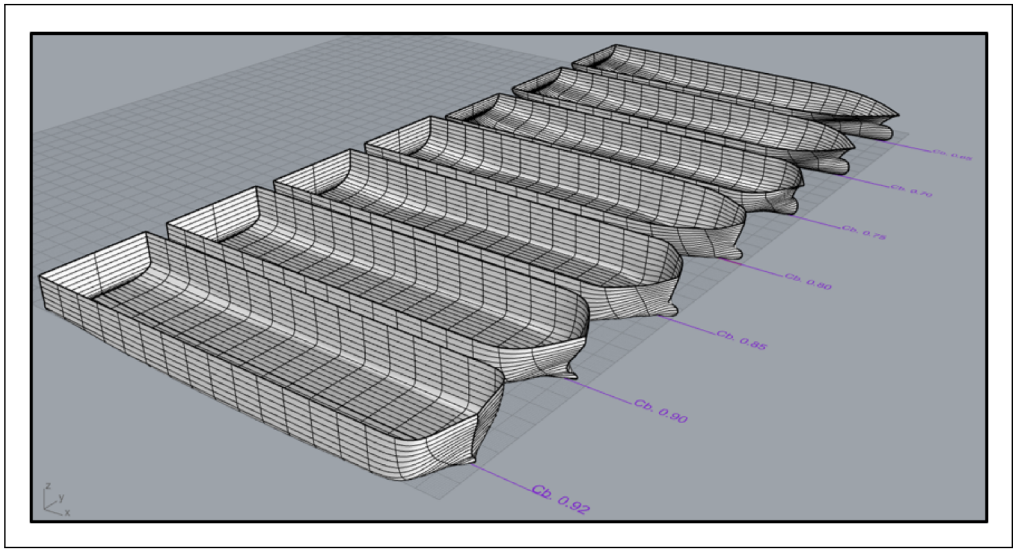

Figure 5. The parent hulls with block coefficients ranging from 0.65 to 0.92.

at the stern along the amidships position, is assumed to provide sufficient space for storing and sea-fastening. A total of 3,024 IDs were developed for the three ID designs.

3.2.3 Parent hulls. Seven parent hulls (Figure 5) were developed, which served as the basis for the automated hull design. The hull surface is generated by considering the full combination of variable ship particulars, fixed particulars, design constraints, ID designs, and parent hulls.

The hydrostatic calculations involved extracting the relevant data describing the hull properties related to stability and hull resistance characteristics in the four loading conditions. The submerged draft of the ID in each loading condition is shown in Table 2.

The hydrostatic tables, consisting of the center of buoyancy of the submerged volume and the hull coefficients in the loading conditions, were calculated using built-in functions in Rhinoceros

Table 2. The submerged draft of the ID in each loading condition, measured from the deck to the mean sea level. Draft of the ID in each loading condition, measured from the deck to the mean sea level.

Condition	Submerged draft [m]
Transit	–
ID submerged	1
ID and TLP submerged	13.7
ID fully submerged	30

ID: installation deck; TLP: tension leg platform.

3D. To draw full GZ curves, the hull surface was inclined at angles of 2°, 5°, 10°, 15°, 20°, 25°, 30°, and 40°, as specified by the International Code on Intact Stability, 2008.[14] To accelerate the computations, the hydrostatic tables of the ID and the ship were generated separately and combined later.

3.3 Ship design module

The ship design module converts geometric hull characteristics into concept ship designs. This involves estimating resistance and power, determining the ballast capacity of both the vessel and the ID, and calculating the vessel's weights and center of gravity. The technical feasibility of the concept designs is validated under various loading conditions, determined by the TLP design and the number of FOWTs on board. The number of TLPs was varied from 1 to 5, with 5 being a reasonable practical limit for the number of fully assembled TLPs to transport with this concept. Four checks are conducted to assess the feasibility of the design, namely: space on deck, deadweight, ballast capacity, and stability. Once the feasibility checks are successfully passed and the workability limits are defined, the design undergoes scenario modeling to assess its performance under various environmental conditions.

3.3.1 Resistance and powering calculation. To calculate the resistance and powering, Holtrop and Mennen's[13] method was used for transit conditions. While the transit speed remains constant for each design throughout the DSE, assuming a uniform speed for the entire fleet could lead to inaccuracies, given the wide variety of designs generated.

To address this issue, a sailing speed relation is implemented based on the block coefficient and waterline length. For the shortest design (with a waterline length of 95 m), a sailing speed of 10 knots (corresponding to a Froude number of 0.32) is assumed, while for the longest design, a sailing speed of 15 knots (corresponding to a Froude number of 0.25) is adopted. In these Froude number ranges, the influence of wave resistance is not governing.[15] Additionally, the range is relatively small, and therefore, a linear profile is adopted for scaling the sailing speed related to the waterline length. These speeds correspond to a reference block coefficient of 0.785, which is the midpoint of the block coefficients of the parent hulls. The scaled sailing speed can now be calculated using,

$$v_{\text{sailing}} = \overbrace{(v_{\text{base}} + (Lwl_{\text{design}} - Lwl_{\text{ref}}) \cdot \text{slope})}^{\text{Linear scaling waterline length impact}} \cdot \overbrace{\left(\frac{1}{1 + (Cb_{\text{design}} - Cb_{\text{ref}})}\right)}^{\text{Scaling for block coefficient impact}} \tag{3}$$

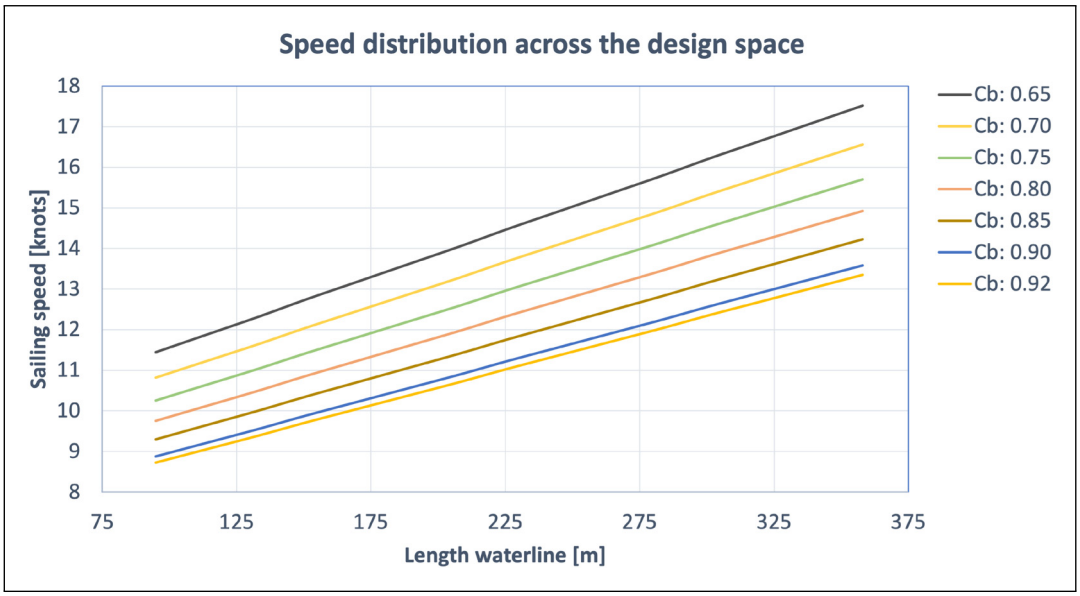

Figure 6. Sailing speed distribution.

where

- v_{sailing} is the scaled sailing speed [ms^{-1}].
- v_{base} is the base sailing speed [ms^{-1}].
- L_{design} is the design length [m].
- L_{ref} is the reference length [m].
- slope is the slope factor [s^{-1}].
- Cb_{design} is the design block coefficient [–].
- Cb_{ref} is the reference block coefficient [–].

The reference waterline length and base sailing speed correspond to values for the shortest design, and the slope is determined by the difference in sailing speeds between the shortest and longest design. From this, the speed distribution among the fleet is depicted in Figure 6.

The required transit speed propulsive power was derived using the method proposed by Klein Woud and Stapersma[16] and the propulsive coefficients from Holtrop and Mennen.[13] The DP conditions of the Windchanger concept are unique, which poses challenges. When lowering the ID, nonlinear flows are created around the structure, and estimating the corresponding loads involves significant complexities. Furthermore, the critical load transfer operation when the FOWT is connected to the tendons and the ID requires a narrow but yet-to-be-determined DP envelope. Finally, during submersion, the ID obstructs the thruster outflow, resulting in significant blind angles. Given these limitations, existing methods are inadequate. Therefore, the maximum propulsive power during DP is estimated using,

$$P_{\text{D;DP}} = P_{\text{D;sailing}} \cdot \alpha_{\text{DP}} \tag{4}$$

Table 3. Efficiency values.

Component	Efficiency (η)
Generator	0.96
Switchboard	0.999
Transformer	0.99
Frequency converter	0.985
Electric motor	0.96

where

- $P_{\text{D;DP}}$ is the maximum propulsive power during DP [kW].
- $P_{\text{D;sailing}}$ is the propulsive power at transit speed [kW], and
- α_{DP} is the DP ratio related to $P_{\text{D;sailing}}$.

The DP ratio, α_{DP}, is assumed to be 70% based on discussions with Allseas Engineering B.V.'s in-house naval architects. This value should be validated in later design stages. Due to the critical installation operations, at least DP2 capabilities are needed, requiring a diesel-electric propulsion system. Typical efficiencies of the system's components, which define the transmission efficiency, were adopted from the works,[17,18] as shown in Table 3.

3.3.2 Ballast capacity estimation—ship's hull. The estimation of ballast capacity is divided into two parts: the ship's hull and the ID. The capacity within the hull is essential to ensure that there is sufficient volume for ballast. The ballast water capacity of the hull is estimated based on the total hull volume provided by the hull generation module. After this, allocations are made for the engine room, fuel and water tanks, and installation mechanism. These allocations are subtracted from the total hull volume to determine the available space for ballast water. The space reservation of the engine room is determined by the empirical relation established by Parson,[19] while the engine room length is calculated based on equation (5),[19] where $Pb_{\text{Installated}}$ is the installed brake power [kW]

$$L_{\text{CM}} = 0.002 \cdot Pb_{\text{Installated}} + 5.5 \tag{5}$$

The required tank volumes for water and fuel are determined based on the design's autonomy and the number of personnel on board. The autonomy is assumed to be 60 days, and the personnel capacity is 50 persons based on in-house assumptions. Additionally, the fuel consumption is estimated based on 85% maximum continuous rating.

To model variations in the vertical center of gravity (VCG) due to different tank filling rates, the total ballast water capacity is divided into shell, double-bottom, and inner tanks. The volume of the shell tank is approximated by multiplying the circumference of the ship's hull by the width of the tank and the depth of the cargo deck. The hull's circumference is estimated using equivalent shapes whose circumferences can be analytically calculated. The volume of the double-bottom tank is estimated based on the empirical relation as defined by Kupras.[20] The inner ballast within the ship is determined by subtracting the volumes of the shell and double-bottom from the total available ballast volume. The VCG of the fuel, water, and ballast tanks was calculated using equation (6), which considers the filling level of the tank and the distance of its bottom from the ship's reference.

$$\text{VCG}_{\text{tank}} = \text{filling} \cdot h_{\text{tank}} + z_{\text{tank;bottom}} \tag{6}$$

3.3.3 Ballast capacity estimation—ID. The total weight, including the TLP, must exceed the combined displacement to submerge the ID since the winch mechanism cannot push the TLP down. Therefore, ballast water is used to adjust the ID's weight. The equilibrium between weight and displacement is described as a function of the draft using,

$$W_{\text{ID;ballast}} = f(z) = (\nabla_{\text{ID}}(z) + \nabla_{\text{TLP}}(z)) \cdot \rho_{\text{sea}} + \text{Load}_{\text{winch}} - W_{\text{FOWT}} - W_{\text{ID}} \tag{7}$$

where

- $W_{\text{ID;ballast}}$ is the required ID ballast weight to submerge to draft z [m],
- $\nabla_{\text{ID}}(z)$ is the displaced volume of the ID at draft z [m^3],
- $\nabla_{\text{TLP}}(z)$ is the displaced volume of the TLP at depth z [m^3],
- $\text{Load}_{\text{winch}}(z)$ is the minimum load on the winch mechanism [t],
- W_{TLP} is the weight of the TLP [t], and
- W_{ID} is the weight of the ID [t].

The winch load component ensures that the winch remains under tension at all times, allowing for active control of the ID during ballast operations and the critical load transfer phase. For the minimum winch load during deck lowering, a standard value of 1,000 tons is adopted. However, due to the complexities involved in the load transfer between the tendons and the ID, a winch load of 2,000 tons is deemed necessary to ensure a safe operation.

The ballast weight on the ID consists of solid and water ballast components. The amount of solid ballast is determined based on the condition where the largest amount of ballast weight is needed, which is when the ID is fully submerged. In this scenario, the entire available space is dedicated to ballast capacity. The solid ballast portion (α_{solid}) is determined by solving,

$$W_{\text{ID;ballast}} = \nabla_{\text{ID}} \cdot \mu \cdot \left(\rho_{\text{sea}} \cdot (1 - \alpha_{\text{solid}}) + \rho_{\text{solid}} \cdot \alpha_{\text{solid}}\right) \tag{8}$$

where

- $W_{\text{ID;ballast}}$ is the total weight of ballast required in the ID [t],
- ∇_{ID} is the volume of the ID [m^3],
- μ is the permeability of the tanks (0.95 for ballast water tanks according to Veritas[14]),
- α_{solid} is the solid ballast ratio, representing the proportion of solid ballast in the total ballast weight, and
- ρ_{solid} is the density of the solid ballast material (4 (t/m^3)).

For the other installation conditions, equation (9) is solved so that the weight of the ID, $W_{\text{ID;ballast}}$, matches the equilibrium as defined in equation (7).

$$W_{\text{ID;ballast}} - W_{\text{ID;solid-ballast}} = \nabla_{\text{ID}} \cdot \mu \cdot \text{filling} \cdot \rho_{\text{sea}} \tag{9}$$

3.3.4 Weight estimation. The weight calculation is based on the methods provided by Watsom[21] and Papanikolaou.[15] Adjustments are implemented to account for the unique features of the Windchanger concept. For example, the ID located at the stern of the vessel requires reinforcements of the hull to cope with the increased longitudinal bending moments. Additionally, the ID itself also comprises a significant portion of the total light ship weight (LSW) due to its proportions and the

presence of permanent solid ballast. To structure the calculation and account for the influence of various ID designs, the LSW is divided into two parts: the ship's hull and the ID, see equation (10).

$$W_{\mathrm{LSW}} = W_{\mathrm{LSW;ship}} + W_{\mathrm{LSW;ID}} \tag{10}$$

The ship's LSW is estimated by categorizing it into three main groups: steel weight, outfitting weight, and machinery weight. To account for the anticipated increased longitudinal bending moments and the additional loads in the aft section due to the interaction between the lowering mechanism and the ship, the steel weight is scaled. Specifically, for the aft 0.5L, the steel weight is increased by 20% to allow for potential reinforcement.

The steel weight is determined by using the equation given by Watsom,[21] which is based on the Lloyds Register's equipment number. The coefficient (K) is assumed to be 0.33, corresponding to general cargo vessels. For the outfitting weight, the method of Papanikolaou[15] has been followed, and a coefficient (C_{outfit}) value of 0.014 ton/m^3 has been assumed. The machinery weight is calculated following the method proposed by Watsom.[21]

The weight of the ID is categorized into three components: steel weight, outfitting weight, and solid ballast weight. It is assumed that the machinery required for the lowering mechanism is included in the ship's machinery weight component. The LSW of the ID is determined based on the weights allocated for the ship and converted into a specific weight per unit length, using equation (11).

$$W_{\mathrm{LSW:ID}} = \alpha_{\mathrm{ID}} \cdot \frac{W_{\mathrm{steel}} + W_{\mathrm{outfitting}}}{L_{\mathrm{hull}}} \cdot L_{\mathrm{ID}} + W_{\mathrm{solid;ballast}} \tag{11}$$

The scale factor α_{ID} accounts for changes in volume per ID design. For the "full design" of the ID (see Figure 4), the scaling parameter is equal to 1, as this shape is similar to that of the conventional stern design of ships. For other designs, α can be calculated using,

$$\alpha_{\mathrm{ID}} = \left(\frac{\nabla_{\mathrm{ID;i}} - \nabla_{\mathrm{ID;full}}}{\nabla_{\mathrm{ID;full}}} + 1 \right)^{2/3} \tag{12}$$

The VCG is estimated using the method proposed by Papanikolaou.[15] To account for variations in depth along the length of the ship, resulting from the increased foredeck height, the corrected side depth (D_s) is used in equation (13).

$$D_{\mathrm{s}} = D + \frac{\nabla_{\mathrm{foredeck}}}{L_{\mathrm{pp}} \cdot B} \tag{13}$$

3.3.5 TLP design and loading conditions. To perform the feasibility checks, the mass, VCG, space requirement, and lateral wind area of the TLP designs are needed as input. For the 20 MW TLP, the total weight is estimated at 7,500 tons with a VCG at 74 m based on in-house assumptions from Allseas. To store this TLP design, 60 m (in the length direction of the ship) of free deck space is required. This number includes a spacing distance between two TLPs of 3 m. The foldable-leg TLP is heavier due to the folding mechanism, estimated at a 5% increase in TLP weight. It is assumed that the VCG remains at the same position. The foldable leg enabled a reduction in space by a factor of 2, being 30 m. This is the minimum distance two TLPs could be stacked. The displacement of the 20 MW TLP at the operational draft is approximately 15,000 tons according to the 3D model.

This means that the required weight to push the TLP down is approximately 7,500 tons. The lateral wind area of a TLP, required for stability calculations, is 3,500 m^2.

3.3.6 Stability calculation. The GZ curve of each design for each loading condition is created based on the hydrostatic output of the hull generation model and the combined VCG. For each loading condition, a maximum VCG is determined based on the criteria outlined in the Code on Intact Stability, 2008[14] to evaluate the ship's stability.

3.3.7 Technical feasibility checks. The technical feasibility checks were conducted sequentially, and a generated concept was considered technically feasible if the following criteria were met:

- Sufficient space onboard to accommodate the TLPs.
- Sufficient deadweight tonnage (DWT) onboard to carry the TLPs.
- Sufficient ballast water capacity on the ship and ID to maintain the desired draft.
- Compliant with the stability criteria in the specified loading conditions.

3.3.8 Workability. In offshore installation operations, workability limits are typically specified using combinations of significant wave heights (*Hs*) and peak crossing periods (*Tp*). The workability model uses time series and the installation procedure as input. In the installation procedure, the *Hs* limits and durations are specified for the suboperations. Based on the workability limits, the model calculates the number of installations ($n_{\text{Inst;tot}}$) that can be completed during the span of the time series ($t_{\text{timeseries}}$). The average workability is calculated using,

$$\text{Workability}_{\text{avg}} = \frac{n_{\text{Inst;tot}} * t_{\text{Inst}}}{t_{\text{timeseries}}} \tag{14}$$

where

- $n_{\text{Inst;tot}}$ is the total number of installations,
- t_{Inst} is the installation time [hours], and
- $t_{\text{timeseries}}$ is the length of the time series [hours].

The analysis is simplified by omitting workability or duration limits between the suboperations. The suboperations are thus treated as unconditional consecutive events. By this simplification, complexities associated with decision-making strategies concerning acceptable time frames and operational limits for on-hold operations are avoided. Currently, it is unknown what the critical conditions are regarding the hydrodynamic behavior, and how this influences the installation mechanism. This introduces significant uncertainties regarding the critical aspect of the operation. These factors lead to the conclusion that establishing the workability limits for each design in a detailed manner is not possible.

Thus, a simplified approach was implemented and applied to the entire fleet. The provided workability limits only concern the *Hs* without specifying details on the corresponding *Ts*. For suboperations that do not include complex tasks demanding high precision, a constant *Hs* is assumed.

A relationship was derived from Guachamin et al.[22] focused on the workability of monopile (MP) and transition piece (TP) installation in the North Sea. This study established workability limits for various wave angles, specifically for TP mating and MP commissioning. An inverse

proportional relationship between the *Hs* and *Tp* limit is observed. The *Hs* limit corresponding to a wave period of 4 s is determined based on the provided *Hs* limits from Guachamin et al.[22] The corresponding linear relation is described by equation (15).

$$Hs_{\text{lim}} = 2.15 - 0.15 * T_s \tag{15}$$

Finally, the number of yearly installations is calculated as the number of workable days per year times the workability for installation divided by the time required per installation, which depends on installation, distance to port, and design-specific parameters such as design speed and deck capacity for in port FAWT loading time (equation (16)).

$$N_{\text{yearly;installations}} = \frac{t_{\text{workable;year}}(0.85 * 8760\,\text{h}) * \text{Workability})}{t_{\text{installation}}} \tag{16}$$

3.4 Economics module

The economics module uses variables that define the design's characteristics to estimate the building costs, which is the basis for the CAPEX and the OPEX. The operational modes determine the fuel costs, which determine the VOYEX. For fuel costs, a fixed cost of €1,000 per ton has been adopted from Ship and Bunker.[23]

For new build costs, a parametric approach was deemed the most suitable method due to the limited available information. In the literature,[21,24,25] the building costs are split up into four main groups. For each group, a specific cost per unit (CPU) is determined based on regression analysis (equation (17)). An additional group is added to account for specific equipment needed for the installation and handling of the TLPs.

$$\begin{aligned} C_{\text{Build}} = {} & \text{CPU}_{\text{Hull}} \cdot W_{\text{Hull}} + \text{CPU}_{\text{Acc}} \cdot n_{\text{Crew}} + \text{CPU}_{\text{Mach}} \cdot \text{Pb}_{\text{Inst.}} \\ & + \cdots + \text{CPU}_{\text{Equipment}} \cdot W_{\text{Equipment}} \end{aligned} \tag{17}$$

For the steel hull, a value of €7 per kg is assumed, which is more accurate for larger ships (hull > 40, 000 tons) than for smaller ones, based on an analysis of the three methods in the literature.[21,24,25] For accommodation costs, a value of €200,000 per crew member is adopted.[24]

The propulsion and machinery group includes all machinery, propulsion systems, electrical systems, and ballast systems. The costs are estimated based on the total installed power responsible for all power generation. For power exceeding 80,000 kW, a value of €1,750 per kW is used. For designs with an installed power of < 40, 000 kW, the average of the output of the equations proposed by Aalbers[24] and Michalski[25] is used. For the in-between values, the average of all methods is taken.

The outfitting and ship's equipment group encompasses all equipment and outfitting on board. All three referenced papers point out that it is difficult to determine the CPU of the outfitting and equipment based on regression. The level of equipment is highly dependent on the ship type, the owner's preference, and the environment the ship is designed for. An average of all methods is adopted for the entire range.

The installation equipment group is added to account for specific on-board TLP equipment, including the lowering mechanism of the ID. A value of 3 million euros per ton of winch load is assumed. This includes all related equipment needed for TLP installation.

Table 4. OPEX distribution.

Component	Value * C_{build}	Portion of OPEX
Labor	2.00%	45%
Insurance	1.00%	20%
Maintenance and repairs	0.75%	15%
Lubrication, oil, paint, and stores	0.50%	10%
Management	0.50%	10%
Total	4.75%	100%

3.4.1 CAPEX. In the maritime industry, the construction of a new vessel is generally financed through a combination of company equity and bank loans. Typically, 40% of the funds come from the company's equity, while the remaining 60% is obtained through bank loans.[24] Based on this finance strategy, the CAPEX of the ship consists of equity, loan repayments, and interest charges. To account for inflation and maintain the net present value of the company's equity, a yearly inflation correction of 2.5% is applied. The inflation rate (Inf_{avg}) represents the average annual inflation rate observed since the 2000s.[26] The loan repayment period is set equal to the expected lifetime of the ship, following a linear mortgage model. Interest rates can vary based on factors such as the company's credit rating and economic conditions.[27] For the analysis, a 5% interest rate is used as a global estimate.[28] The total costs of the CAPEX was determined using equations (18), (19), and (20).

$$C_{\text{CAPEX}} = C_{\text{Equity}} + C_{\text{Loan}} \tag{18}$$

$$C_{\text{Equity}} = C_{\text{build}} * \left(40\% * (1 + \text{Inf}_{\text{avg}})^{t_{\text{Life}}}\right) \tag{19}$$

$$C_{\text{loan}} = C_{\text{build}} * (60\% + C_{\text{Interest}}) \tag{20}$$

The OPEX estimation is based on Aalbers.[24] The OPEX components are taken as a percentage of the building costs and are on an annual basis, Table 4 and equation (21).

$$C_{\text{OPEX}} = 4.75\% * C_{\text{build}} \tag{21}$$

VOYEX comprises fuel costs and other voyage-related expenses, such as harbor fees and pilotage charges. In the model, the fuel costs are calculated per design based on the power demanded to reach its sailing speed. It is assumed that 75% of the VOYEX are fuel costs and the remaining 25% are other voyage-related costs.[29] The total costs per TLP installation are calculated by using the CAPEX, OPEX, and VOYEX using,

$$C_{\text{Inst;concept}} = \frac{C_{\text{CAPEX}}}{n_{\text{Inst;life}}} + \frac{t_{\text{Life}} * C_{\text{OPEX}}}{n_{\text{Inst;life}}} + C_{\text{VOYEX}} \tag{22}$$

4 Results

This section explores the results of the DSE covering both the technical feasibility of the vessel's design and the cost-effectiveness across various operation scenarios.

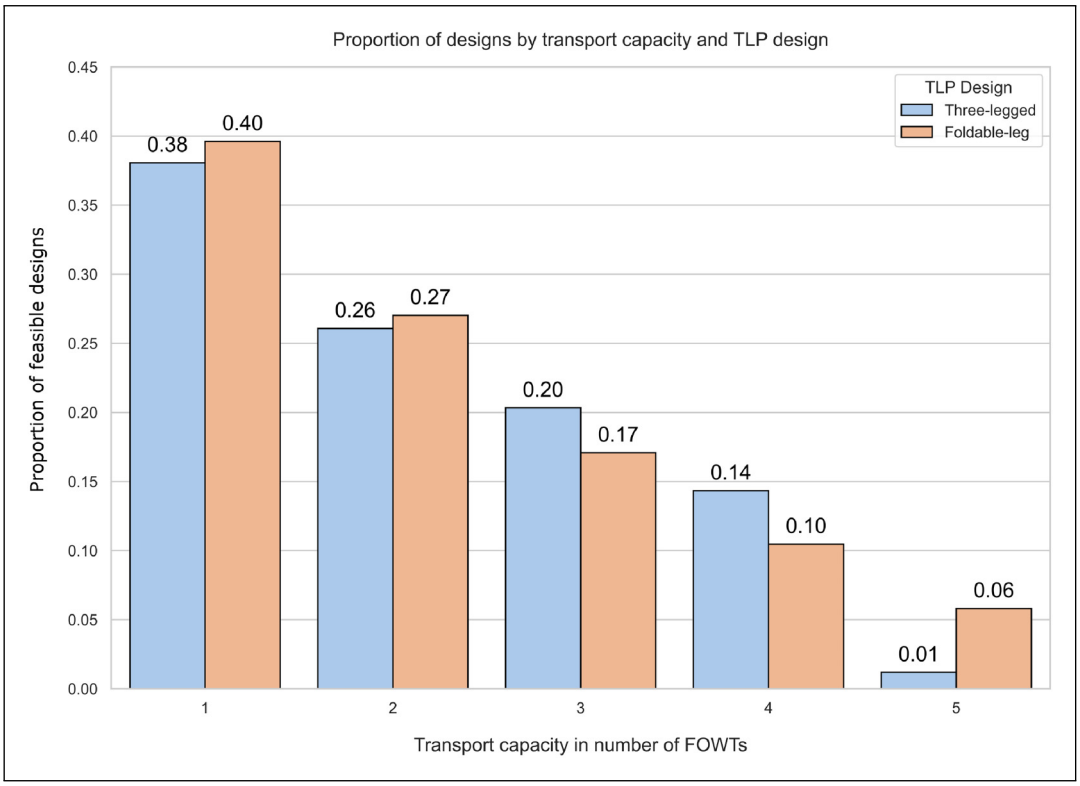

Figure 7. Distribution of the transport capacity per tension leg platform (TLP) design of the design space.

4.1 Technical feasibility results

The support visualization and interpretation of results, the results are categorized into four areas:

(1) **General feasibility bounds**: Identifies the limiting factors based on feasibility checks, and which loading conditions are deemed the most critical.
(2) **Ship-specific feasibility bounds**: Highlights the design variables' impact on the dominant feasibility bound.
(3) **ID design**: Provides insights into variables that influence the design of the ID.
(4) **Design interaction**: Here all areas are explored to understand their interaction.

All plots categorize the designs based on transport capacity per TLP design. The transport capacity is defined as the maximum number of TLPs it can carry. The distribution of feasible designs within the fleet, relative to their transport capacities, is presented in Figure 7. The number of feasible designs (approximately 220,000) for a three-legged TLP represents about 75% of the design space. For a foldable TLP, this number is slightly lower, at 72%.

As the transport capacity increases, the number of designs capable of accommodating a higher number of TLPs decreases proportionally. This pattern aligns with expectations, as a higher transport capacity demands greater capabilities of the design, resulting in fewer feasible solutions.

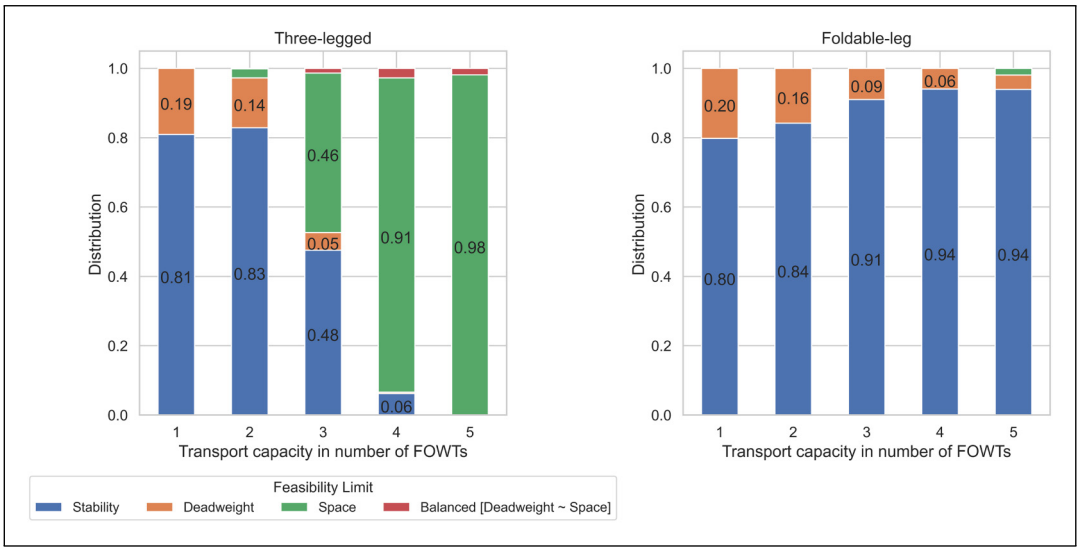

Figure 8. General feasibility bounds per tension leg platform (TLP) design.

Notably, for transport capacities of 4–5 TLPs, a shift is observed in the distribution per TLP design, while the total number of designs present in those bins remains similar.

4.2 *General feasibility bounds*

The general feasibility bounds include considerations such as space requirement, DWT requirement, ballast capacity requirement, and compliance with stability criteria. To visualize which factor is limiting, stacked normalized bar plots are used (see Figure 8). These bars are interpreted as: for designs with a particular transport capacity, what is the limiting criterion for being one unit higher?

The absence of the ballast capacity requirement in the bar plots suggests that each design adequately meets this criterion. In the graphs, three regions can be identified:

(1) **Transport capacity 1–2**: When comparing both TLP designs, it appears that the impact of the TLP design itself is not significant. For both configurations, the design is driven by stability limitations. As a result, space and DWT are non-limiting factors. A contributing factor may be the height of the VCG, which primarily limits stability, despite the cargo not being particularly heavy.

(2) **Transport capacity 3**: A shift is observed where the space requirement starts to play a significant role. Storing multiple TLPs necessitates a relatively large ship, which provides a stability margin. However, when this space requirement is decreased with a foldable TLP, stability remains a challenge.

(3) **Transport capacity 4–5**: For the three-legged TLP, nearly all designs are constrained by space. Designs accommodating more than 3 TLPs are of significant proportions, reducing stability concerns. This can be attributed to the exponential increase in the design's displacement compared to the linear increase in the number of TLPs. This is due to the vessel length being determined based on the required deck space, and the max beam of the design

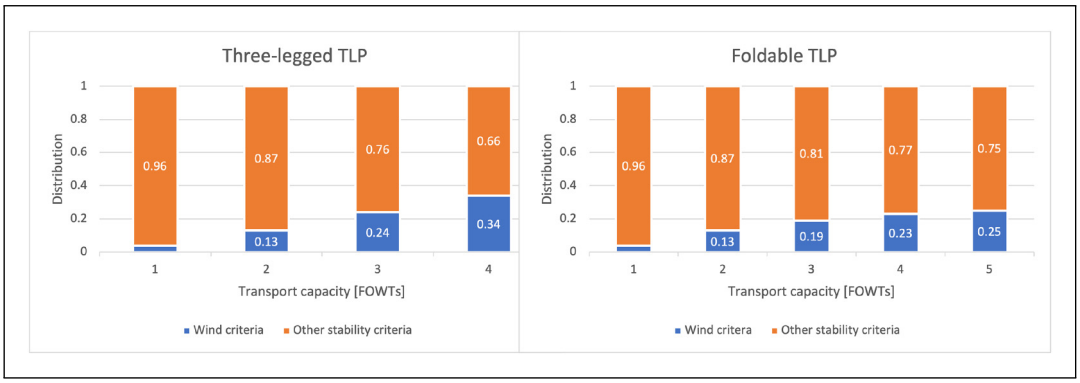

Figure 9. Distribution of critical conditions.

depends on the L/B limitation of Holtrop and Mennen.[13] Thus, longer vessels are also subsequently wider, causing the increase in displacement and stability margin. Additionally, to account for the weight of the extra ship section to accommodate an extra TLP is relatively large compared to the weight of the TLP, contributing to a lower combined VCG. For the foldable-leg TLP, the stability limit becomes even more prominent.

These plots show the significant impact of the TLP design on the vessel's feasibility bounds, particularly when designed for higher transport capacities. The considerable reduction in space requirements for foldable-leg TLPs shifts the focus toward stability as a key design criterion. It can be questioned whether a foldable-leg TLP is desirable, as the space saved by folding a leg is not efficiently utilized. Furthermore, unfolding a complete leg is challenging due to its particularly large mass and dimensions.

4.2.1 Limiting stability conditions. The results also indicate that meeting stability criteria poses a challenge. Stability is examined in the four loading conditions. Results showed that the IMO wind criterion leads to unrealistic outcomes. These regulations prescribe wind calculations at speeds exceeding 60 knots from the side, a condition that is not encountered by offshore installation vessels at sea. This is because it is extremely impractical to design offshore installations such that they can withstand IMO wind loads due to the criticality of the operation. Therefore, operations are carefully planned to avoid severe weather conditions, and vessels will typically seek shelter or postpone activities if extreme winds and waves are predicted. TLP installation is a restricted operation, constrained by weather windows and operational limits well below the IMO wind criteria. To address this, the following approach is applied: first, the minimal wind speed limit is set equal to the in-port FAWT assembly limit, which is 10 m/s.[30] For this wind speed, compliance with the IMO intact stability criteria is verified. Designs that fail to meet these criteria at this wind speed are deemed infeasible. Subsequently, the actual wind limit of each design is used as an input for the workability calculation.

Figure 9 shows the distribution of the limiting stability criteria. If the other stability criteria are limiting, the wind criterion is, by definition, also limiting due to the interpretation of a GZ curve. If the wind criterion is limiting, the design is not able to withstand wind speeds above 10 m/s but complies with the other stability criteria.

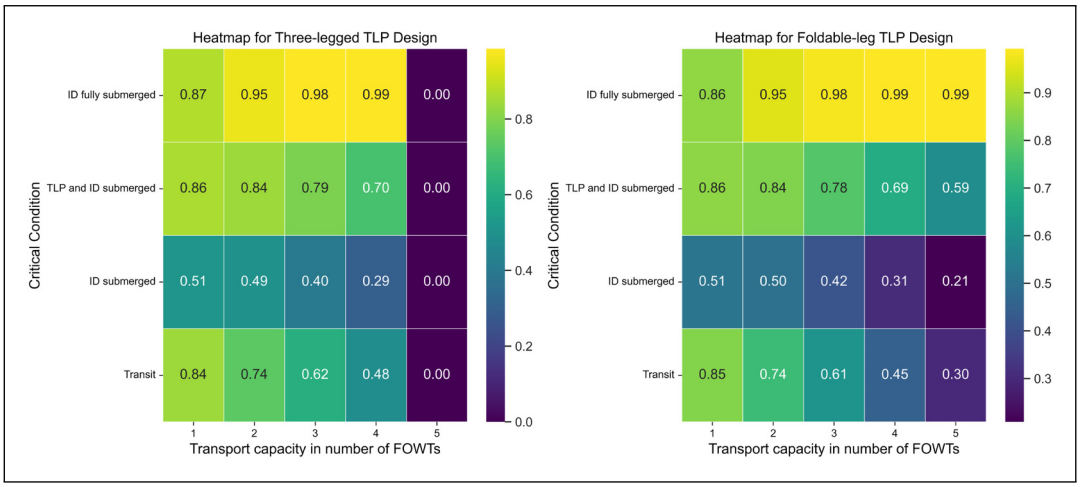

Figure 10. Critical conditions.

It was observed that for higher transport capacities, the influence of the wind limit becomes more pronounced, which is due to the increased lateral wind area. The wind area criterion is calculated in the transit condition, as it represents the largest lateral area. Figure 10 displays the distribution of limiting conditions for each TLP design. It provides a breakdown, showing the percentage of cases in which a particular condition acts as the limiting factor. Note that the proportion exceeds 1 because more than one condition can be limiting at the same time. The fifth column of the three-legged column is empty because stability is not limiting for this bin.

The ID fully submerged condition emerges as the most critical loading condition for both TLP designs, particularly for transport capacities exceeding 1. For larger designs, this condition becomes even more critical. This is unexpected as the proportion of submerging volume decreases for larger designs; however, this reduction does not appear to significantly affect technical feasibility. One possible explanation is that the overall stability of these designs is inherently more critical, as increasing ship size does not necessarily translate into improved stability.[15]

Notably, the occurrence of the ID submerged condition as a limiting factor is significantly lower than that of other conditions. This could be clarified by considering that in this condition, the legs intersect with the waterline, and the moment of inertia of the waterline contributes positively to the stability.

4.3 *Ship-specific feasibility bounds*

4.3.1 Impact of length raised foredeck. For each deck length, a variant with a short and long raised foredeck is analyzed, while keeping the other parameters constant except for the length overall and displacement. The additional bow length is reflected in the overall length, leading to an increase in displacement. This study aims to examine whether this is an effective approach to increase the transport capacity for stability-bounded designs. Due to the raised foredeck, the inclination angle at which the side of the deck floods occurs at greater angles, which is typically a point of stability loss.[15] Figure 11 shows that the impact of bow length is negligible for both TLP designs. For larger transport capacities, there is a slight preference for designs with a long bow design, presumably

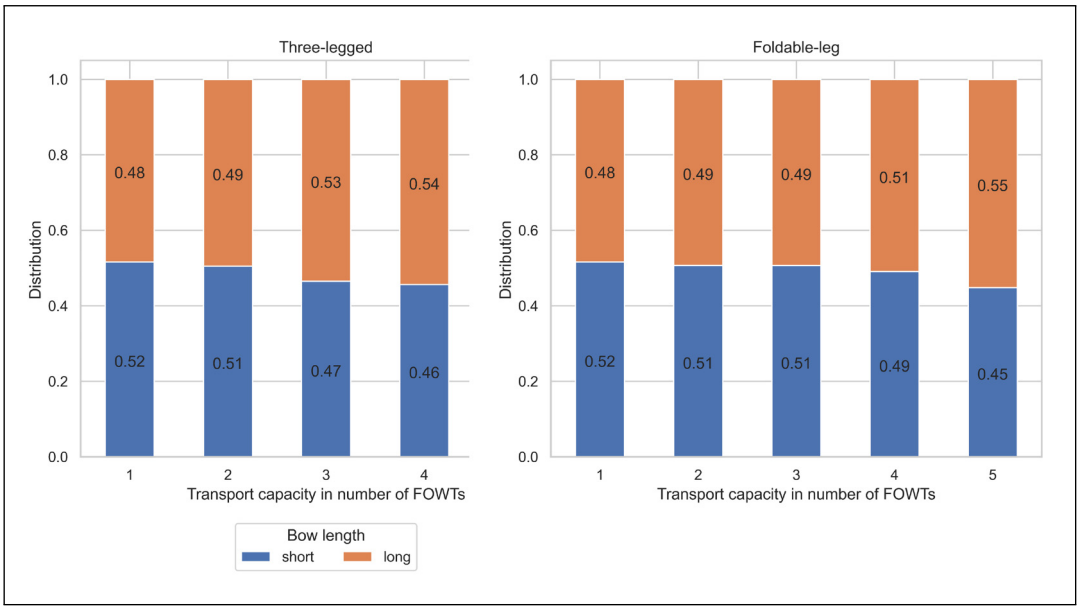

Figure 11. Bow length impact.

due to the added displacement, which slightly lowers the combined VCG. It is thus concluded that enlarging the bow is undesirable as it does not significantly influence technical feasibility.

4.3.2 Impact of ID design. The three ID designs were assessed as to their impact on the ship's technical feasibility for stability-constrained designs (see Figure 12). The impact of the fullness of the ID appears to be relatively insignificant. This limited impact may seem contradictory, given that the ID's buoyancy directly affects stability calculations. However, during this DSE, the ID mechanism is modeled as a winch system, requiring a minimum negative buoyancy of 1,000 tons in submerged conditions. Consequently, this assumption results in less influence on the submerged volume, as the ballast water intake needs to compensate for the extra buoyancy, resulting in a small net effect on stability. The slight preference for a fuller ID design as the transport capacity increases might be explained by the fact that the fully submerged condition becomes critical. Fuller designs tend to be heavier, thereby lowering the combined VCG when the ID is submerged to greater depths.

4.3.3 Impact of variable ship design parameters. The analysis of general feasibility highlighted stability and space as the main limiting factors, depending on the TLP design and transport capacity. Three different regions were observed. Figure 13 summarizes these results, containing only the designs' displacement, showcasing the impact across the dataset. The findings indicate:

(1) **Transport Capacities 1–2**: No significant differences were observed in the feasibility bounds. This indicates that the total displacement of the designs is identical, confirming that the TLP design has minimal influence within this range.

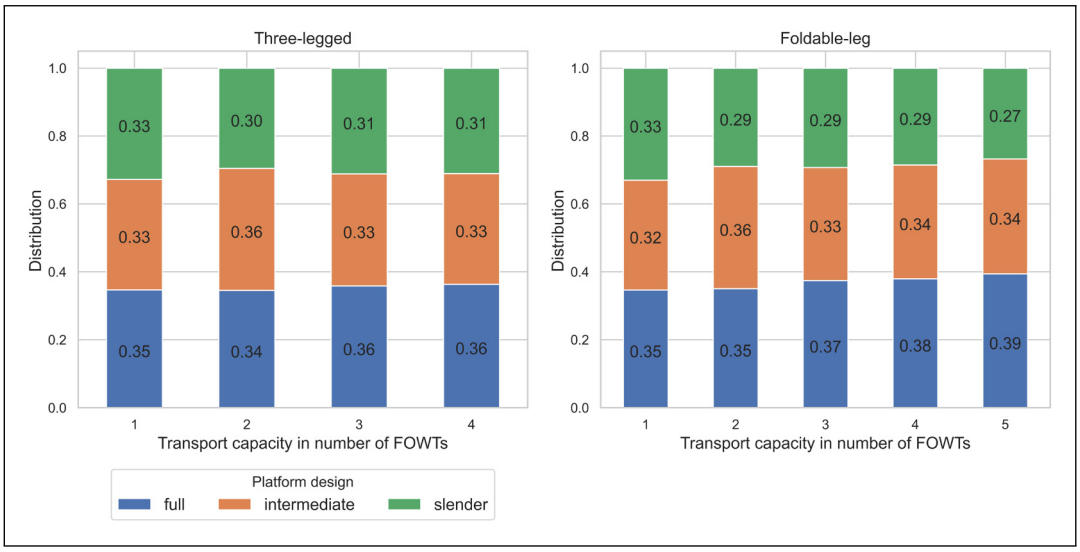

Figure 12. Installation deck impact on stability.

(2) **Transport Capacity 3**: The three-legged TLP design begins to experience space limitations. The increased space requirement of three-legged TLPs appears to be reflected in larger vessels with an increase in total displacement.
(3) **Transport Capacities 4–5**: The three-legged TLP configuration is significantly constrained by space requirements. The resulting designs exhibit even higher displacement, further emphasizing the influence of space constraints.

It is thus concluded that the impact of the TLP design on technical feasibility is limited for ships with lower transport capacities (< 3). However, for larger transport capacities, the TLP design does influence technical feasibility. The lower displacement indicates that in these cases, a foldable-leg TLP is advantageous strictly from a displacement perspective.

4.4 Interaction ship design—ID design

The design of the ID and winch mechanism is mainly determined by two main factors: the winch load and the ballast water intake. A higher winch load results in a more complex and expensive system, while the ballast water intake influences the installation since pumping large amounts of water is time-consuming.

4.4.1 Design conditions ID. During the installation procedure, the buoyant forces and mass of the ID, ballast water, and TLP need to be balanced to ensure that the minimum required winch load is maintained. To identify the determining conditions for the design winch load and the ballast water intake, each step of the installation procedure is analyzed. Figure 14 is used to illustrate the ballast water intake and winch tension during the installation procedure in general. The design used for this illustration is not a Pareto optimal solution, but just a design in mid-design space. The intake of ballast water reaches its maximum when the ID is fully submerged. For the winch load, the transit

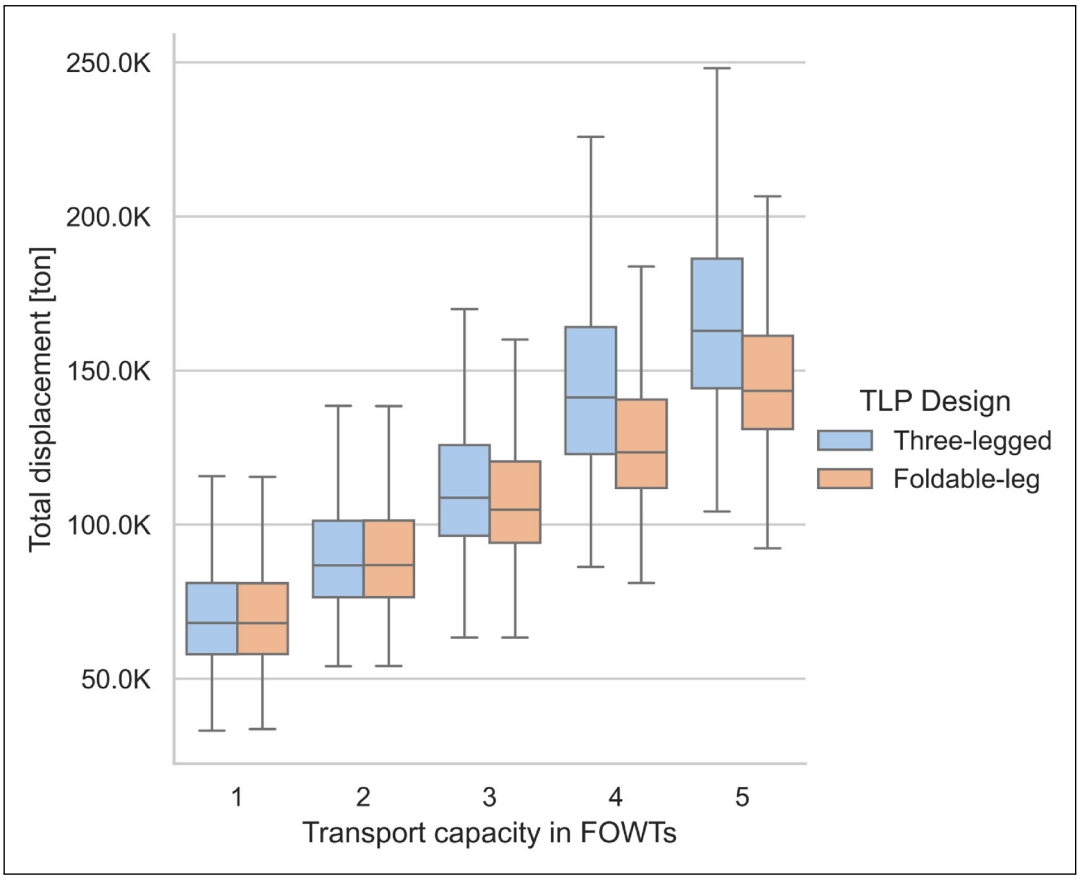

Figure 13. Boxplot total displacement per tension leg platform (TLP) design and transport capacity.

condition predominates. This is primarily due to the weight of the TLP and the ID, which is only partially countered by the displacement of the ID as the draft is limited in this condition.

4.4.2 Design Pareto front identification. Figure 15 shows tradeoffs between wind load and ID ballast capacity. The distance from each point to the Pareto front is illustrated using the color map, and is calculated as the vector toward the closest point of the Pareto front. A notable outlier is observed, positioned just below a winch tension of 7,500 tons and a ballast water capacity of 20,000 tons. The design properties corresponding to this point are presented in Table 5. This point distinguishes itself as it lies on the boundary of the design space. The draft and depth are at their maximum. The beam is on the high side and relatively close to the maximum of 75 m. The displacement in transit and the total weight of the ID are properly balanced. As a result, the winch load is primarily determined by the weight of the TLP. Additional discretization around this outlier was not deemed necessary, as the primary goal of this study was DSE (as opposed to design optimization) in order to identify the high-level key design trends and drivers to be used in later stages of concept development, where these are worked out in more detail.

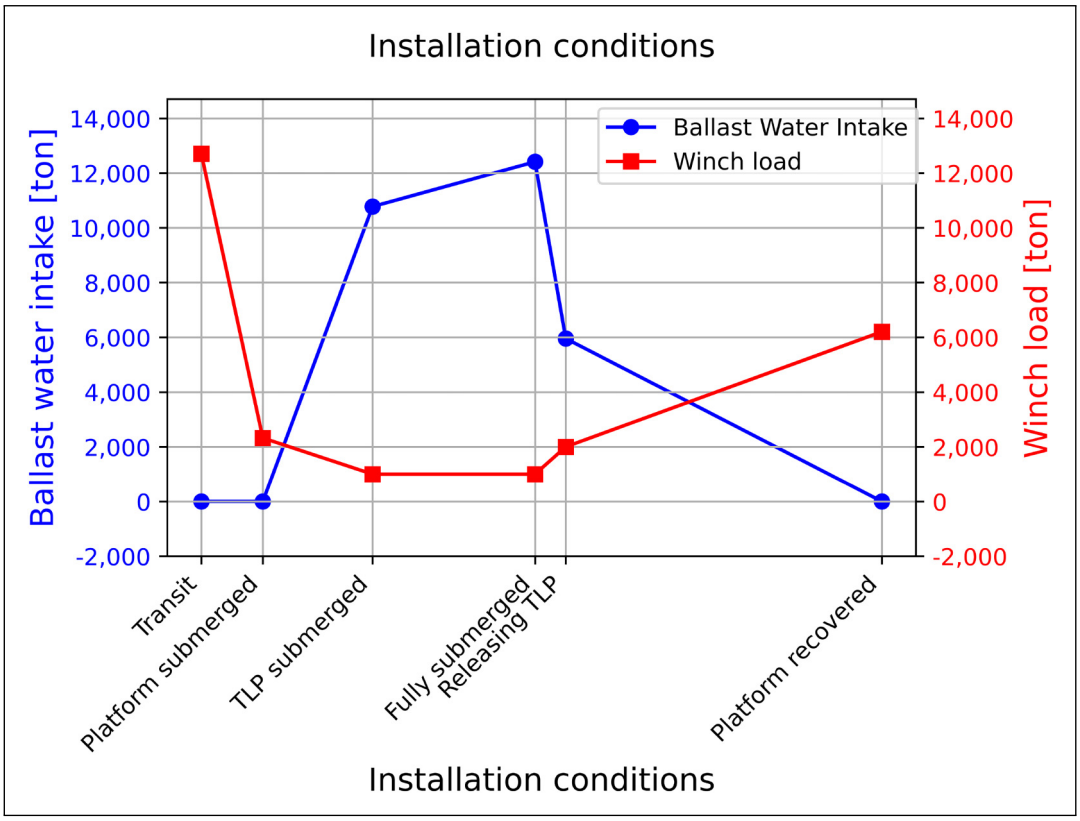

Figure 14. Installation conditions for installation deck design.

4.4.3 Design variables. The impact of draft, beam, depth, and displacement on the Pareto front is shown in Figure 16, with the identified outlier highlighted with dots. The shaded area encompasses all designs within the design space, while the lower line represents the Pareto front. It is important to note that each point in the red-shaded area corresponds to another point in the blue-shaded area, allowing for independent selection of the design point.

The displacement during transit plays an important role in both the ballast water intake and winch load of the ID. Within the mid-range of displacement, a linear relationship for both design factors is observed. For depth and draft, this linear behavior extends across the entire range, with outliers occurring at the boundaries of the design space. In contrast, the influence of the beam appears to be less pronounced, suggesting it may be of lesser importance, opening up the possibility of considering an ID smaller than the vessel itself. When designing the ID solely from its perspective, a tradeoff emerges between the ballast water intake and winch load. This research suggests that the impact of winch load outweighs that of ballast water intake.

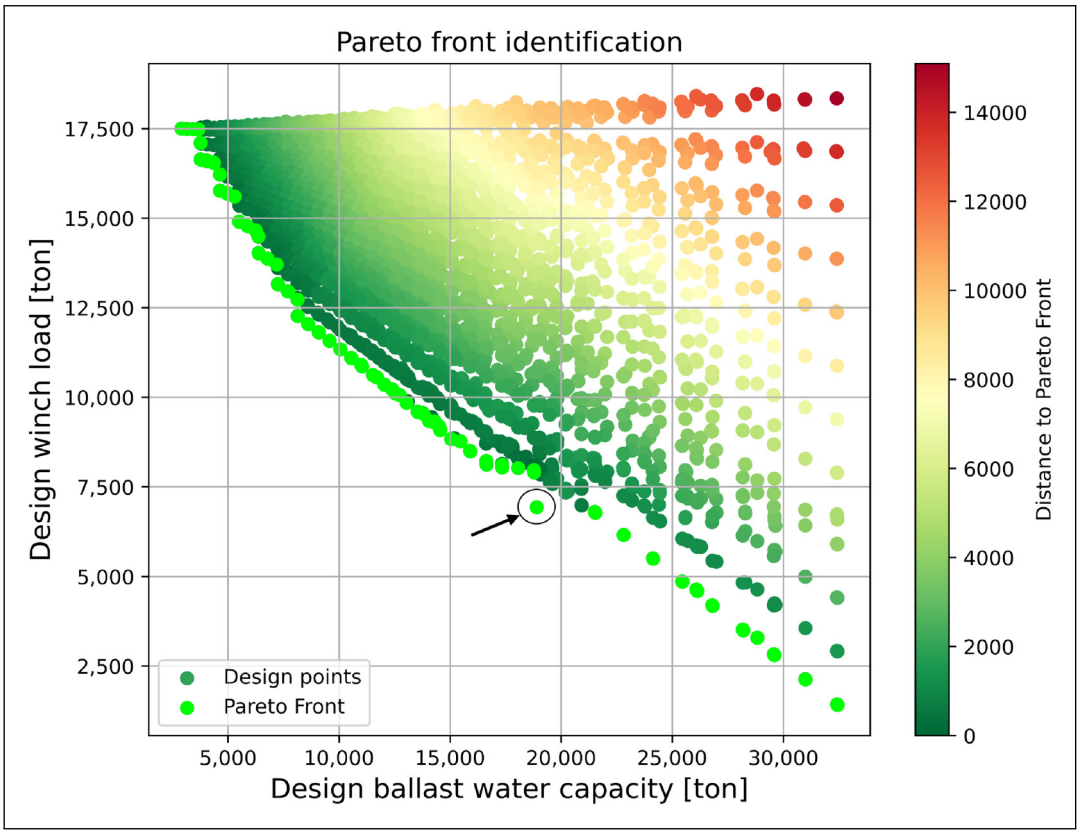

Figure 15. Installation deck (ID) Pareto front.

5 Cost-effectiveness results

To assess the economic performance, two distinct areas are evaluated: the North Sea and the U.S. East Coast (see Table 6). This section evaluates the performance across the two demonstration environmental areas, varying distances to the port, and two TLP designs. With over 300,000 solutions in the design space, two areas, two TLP designs, and eight different distances to ports, there are approximately 10 million configurations. Due to this large design space, detailed workability analyses were not possible. Consequently, smaller ships are favored due to the equal operational limits across all designs. This obscures whether larger ships justify their increased costs through increased workability. Despite these simplifications, the analysis still offers insights into the influence of different scenarios on the installation costs of FOWTs.

5.1 Impact operational area and distance to port

Figure 17 visualizes the impact of distance to the port for both operational areas on installation and the number of yearly installations. The blue lines represent the results of the top 2.5% performing designs for the North Sea, while the orange lines depict the results for the U.S. East Coast. The smooth appearance of the curve can be attributed to the large number of design configurations evaluated. While small cost discontinuities do occur when switching between optimal designs,

Table 5. Installation deck design.

Parameter	Value	Unit
Beam	67.5	m
Draft	12.0	m
Depth deck	18.0	m
Installation deck (ID) volume	21,220	m^3
Solid ballast	6,870	ton
Displacement transit	10,610	ton
Total weight	11,300	ton
Design winch load	6,930	ton
Design ballast water capacity	18,900	ton

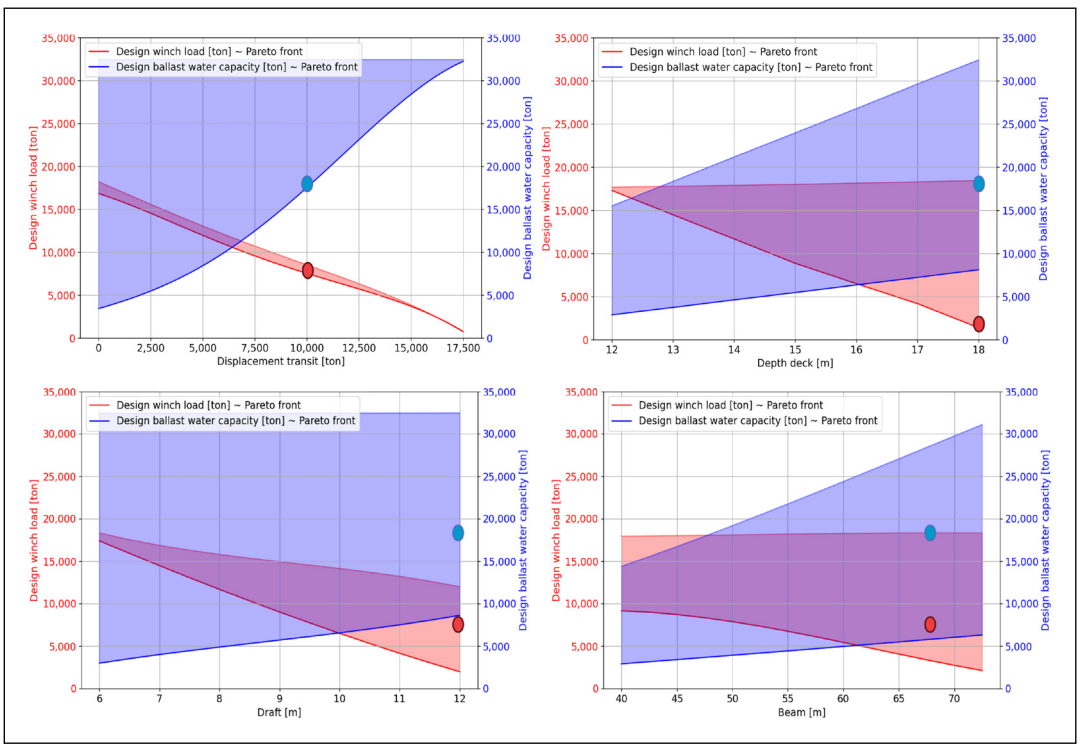

Figure 16. Installation deck design parameters.

they are not visually prominent. The costs (left graph) of installation calculated using equation (22) for the North Sea are nearly twice as high as those for the U.S. East Coast. Based on the number of yearly installations (right graph), it can be concluded that this difference is the result of the reduced workability due to challenging wave-wind conditions. Given that workability is almost half, while the average wave height in the North Sea is only approximately 25% higher, this suggests that the sensitivity of the defined workability limits on the overall cost-effectiveness is significant.

The graphs of both areas for the range of distances to shore show a similar behavior with only a shift along the *y*-axis. This is attributed to the absence of wave spectra, as only wave height and

Table 6. Average environmental conditions.

Location	Average		
	Significant wave height (m)	Peak period (s)	Wind speed (m/s)
North Sea	2.1	8	8.6
U.S. East Coast	1.4	7.5	10

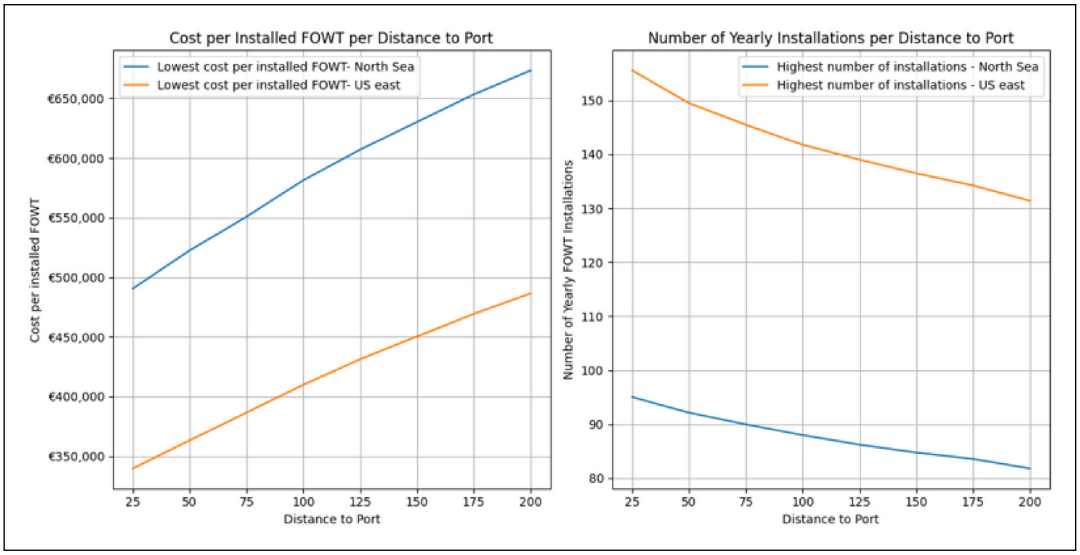

Figure 17. Impact of the operational area and the distance to shore on the design's performance.

weather window are considered. The lower significant wave heights in the U.S. lead to increased workability; however, in areas with more swell, this is not necessarily the case.

5.2 *Impact of the transport capacity*

Figure 18 shows the impact of the transport capacity and distance to port on the normalized cost per installation. The costs have been normalized so the lowest value is set as the baseline and normalized to 1. This allows for a direct comparison of performance between configurations. For example, a value of 1.2 indicates a 20% increase in cost or annual installations compared to the baseline. This indicates that for nearshore wind farms under 100 NM, the transport capacity of 1 TLP performs 10%–20% better than a transport capacity of 2, while the number of yearly installations is significantly lower. This indicates that to justify the increased costs of larger ships, a significant portion of the installation time must be dedicated to transit conditions. However, it cannot directly be stated that the design with a transport capacity of 1 is the better choice. Completing a project in less time also adds value, which is not quantified during this analysis.

The analysis also shows that for wind farms located between 100 NM and 200 NM, the transport capacity has only a minor impact on the number of yearly installations. The additional time required for skidding operations for higher transport capacities seems to balance with the reduction in transit time per TLP. However, this highlights a flaw in the model, as the installation cycle of ships with

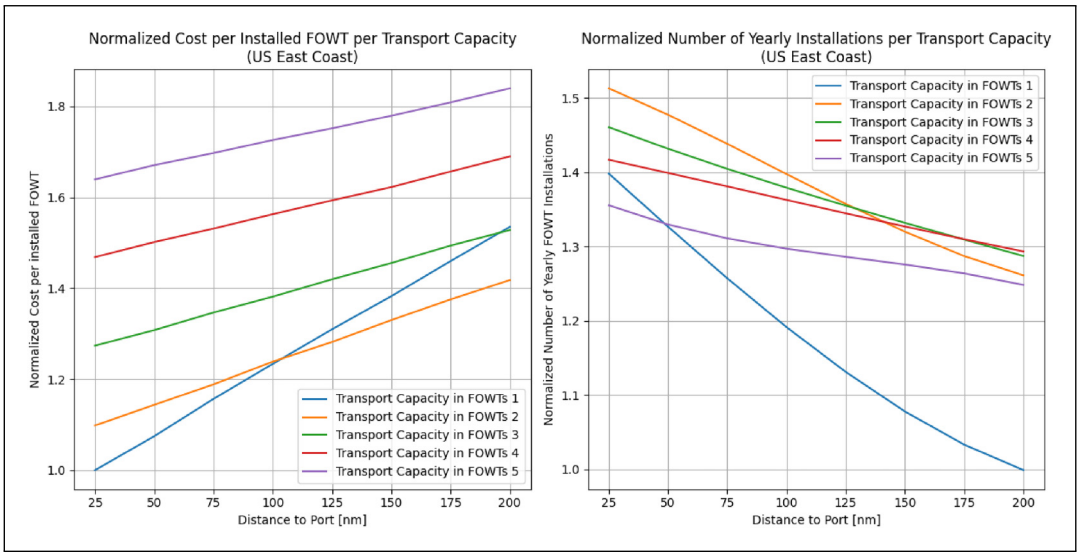

Figure 18. Impact of the transport capacity and the distance to shore on the design's performance.

higher transport capacity is longer, negatively impacting workability. This effect has not been fully considered in the model. The normalized costs of designs providing transport capacities above 2 are inherently higher due to the increased expense of larger vessels, considering the similarity in the number of installations during their lifetime.

5.3 Impact of the TLP design

Figure 19 shows the impact of TLP design and transport capacity for nearshore and far-offshore, indicating that for transport capacities exceeding 3, the foldable-leg TLP emerges as the more cost-effective option. This finding aligns with the results of the technical feasibility analysis, which indicated that the designs for larger three-legged TLP cargo capacities are constrained by space limitations. For smaller ships, the TLP design has minimal influence on ship design, as evidenced by these results. The drop observed in the far-offshore configuration at a transport capacity of 2, because this is the most cost-effective configuration, following Figure 18.

5.4 Impact of the ID design

Figure 20 illustrates the performance of various ID designs. A fuller design emerges as the preferred option for cost-effectiveness for both distance-to-port configurations. Results show that the decrease in winch load resulting from a higher displaced volume during transit offsets the additional material costs. Additionally, the difference is more pronounced at the boundaries of the transport capacity range. As various factors, including weight, winch load, and stability, contribute to determining the cost-effectiveness of the ID design, this complexity makes it challenging to pinpoint the main cause. However, for a transport capacity of 5, the technical feasibility analysis showed a slightly more pronounced preference for the "full design" of the ID (see Figure 4) due to its positive impact on stability.

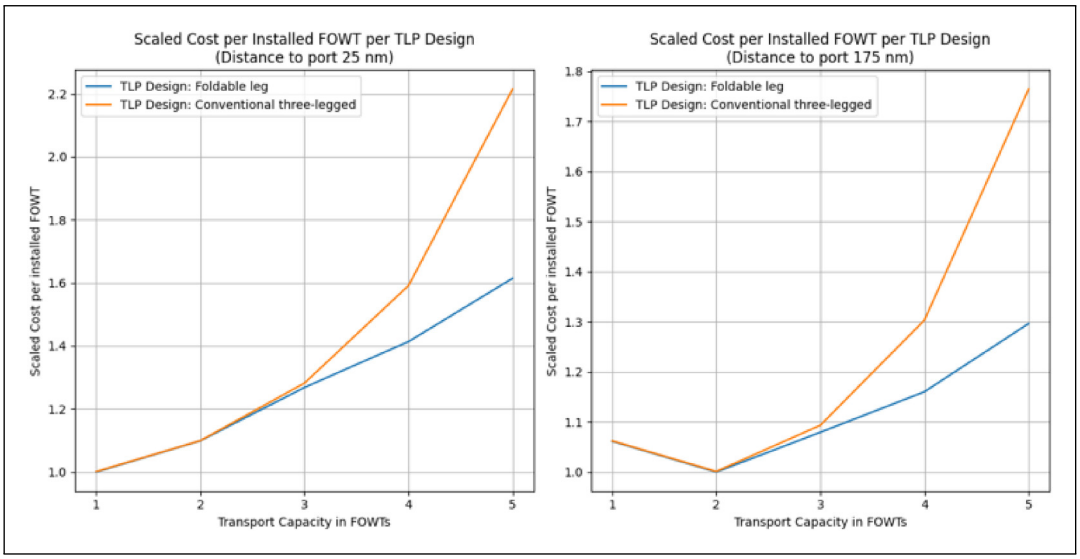

Figure 19. Impact of the tension leg platform (TLP) design and the transport capacity on the design's performance.

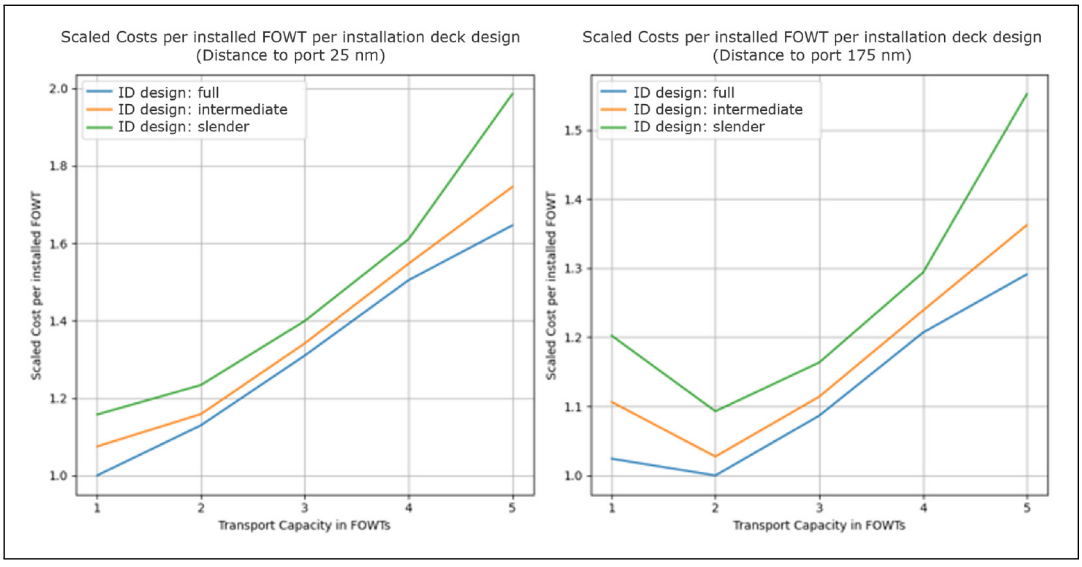

Figure 20. Impact of the installation deck design and transport capacity on the design's performance.

5.5 *Optimal design ranges*

The optimal design ranges depend on various scenarios. For this analysis, the top 2.5% performing designs for each configuration are filtered based on the cost of installation. From this selection, the lower and upper bounds of the design range are established, determined by the lower quartile (25%) and upper quartile (75%). Table 7 presents the design ranges for various domains. The draft and block coefficient are not shown because the optimal draft consistently falls between 8 and 10.5 m,

Table 7. Design ranges for different scenarios.

Area	Distance to port [NM]	Cost per installation	Yearly TLPs	TLP count	*L* [m]	*B* [m]	*D* [m]
N. Sea	25–75	€490k–€515k	77	1	188–208	47.5–55.0	15–17
N. Sea	75–125	€565k–€600k	81	2	189–208	50.0–62.5	15–17
N. Sea	125–200	€610k–€645k	78	2	208–227	52.0–62.5	16–18
N. Sea	150	€590k–€620k	80	2	189–227	50.0–62.5	15–17
U.S.	150	€420k–€445k	126	2	189–227	50.0–62.5	16–18

TLP: tension leg platform.

Table 8. Design ranges for different scenarios for distance to port 150 NM.

TLP design	T.C.	Cost per installation	Yearly TLPs	*L* [m]	*B* [m]	*D* [m]
Three-legged	4	€1530k–€1730k	83	338–360	62.5–72.5	15–17
Foldable-leg	4	€1270k–€1585k	83	295–358	60.0–70.0	15–17
Three-legged	5	€1710k–€1845k	80	358–358	67.5–72.5	15–17
Foldable-leg	5	€1515k–€1740k	80	317–358	65.0–72.5	15–17

TLP: tension leg platform.

and the block coefficient ranges from 0.75 to 0.85 across all scenarios. Designs with transport capacities of 1 to 2 emerge as the most cost-effective solution in these scenarios. Interestingly, the TLP design does not significantly influence cost-effectiveness in these cases.

When a ship designer opts for larger transport capacities, despite potential cost implications, the choice of TLP design becomes a significant factor (see Table 8). The draft for these designs ranges between 7 and 9.5 m, while the block coefficient of 0.92 is optimal.

6 Conclusions

This research presented a DSE of a novel TLP installation vessel. A model was developed that assesses areas impacting technical feasibility and economic effectiveness. The research showed that for smaller transport capacities of 1–2 TLPs, stability is the primary factor affecting technical feasibility, regardless of the TLP design. However, for capacities of 4–5 turbines, the foldable-leg TLP resulted in significantly shorter designs with lower displacement. This leads to the conclusion that in the transport and installation of fully assembled FOWTs, the VCG height in relation to its footprint determines the technical feasibility boundary, with DWT not being a concern. The fully submerged condition, along with wind criteria, emerges as the most critical loading scenario. Increasing displacement of the ID during transit is the most effective strategy to reduce the winch load of the ID. The model underscores the benefits of a voluminous ID design from a technical feasibility standpoint. Furthermore, the winch system proves advantageous, positively influencing stability by shifting the combined VCG downward, particularly in fully submerged conditions.

The model proved capable of evaluating the cost-effectiveness of designs across different scenarios. Designs with lower transport capacities demonstrate superior performance, leading to the conclusion that a foldable-leg TLP is not a desired innovation for the considered scenarios. The influence of TLP design on cost-effectiveness becomes apparent at transport capacities of 4 and 5 turbines. However, the optimal transport capacity is 2 for wind farms with a distance to shore

between 100 and 200 NM. For nearshore farms below 100 NM, designs with a transport capacity of 1 offer the lowest installation costs, despite a significant reduction in the number of yearly installations. This underscores the importance of assessing the value of time, which is currently not evaluated in the model. The overall results show that the Windchanger concept has the potential to be a robust and cost-effective installation solution.

7 Future work

While the Windchanger concept shows promise, further development is required to realize its full potential. First, higher-fidelity analyses are required in the areas of stability, powering (both for resistance and DP), and workability to validate the assumptions and results developed during this concept exploration activity. These higher-fidelity analyses come at higher computational costs, and thus, a proper balance should be found between concept exploration and optimization. Second, additional details regarding costs and the detailed design of the ID, skidding mechanism, sea-fastening, winch-lowering system, and control system would improve the accuracy of the economic analysis. Third, the duration of each installation step should be modeled at a higher fidelity in later steps of the design process. Finally, it is important to note that the findings of this study may not directly extend to smaller FOWTs, as factors such as the TLP's footprint, VCG, and weight significantly influence technical feasibility. The scalability of the Windchanger concept needs to be studied to account for the development path of floating wind technology over the coming years.

Acknowledgements

This research was performed at the Department of Maritime and Transport Technology at Delft University of Technology,[31] and the authors would like to acknowledge Delft University of Technology and Allseas for their support of this research.

ORCID iDs

Jesse J Flierman https://orcid.org/0009-0001-5708-5741
Austin A Kana https://orcid.org/0000-0002-9600-8669

Author contributions

Jesse J. Flierman: Conceptualization; Investigation; Methodology; Software; Writing – original draft; Writing – review & editing.
Vera C. Terlouw: Conceptualization; Supervision; Writing – review & editing.
André L.J. Steenhuis: Conceptualization; Supervision; Writing – review & editing.
Austin A. Kana: Conceptualization; Interpretation of data; Supervision; Writing – original draft; Writing – review & editing.

Funding

The authors received no financial support for the research, authorship, and/or publication of this article.

Declaration of conflicting interests

The authors declared the following potential conflicts of interest with respect to the research, authorship, and/or publication of this article: Austin A. Kana is an Editorial Board Member of this journal, but was not involved in the peer-review process nor had access to any information regarding its peer-review.

Supplemental Material

Supplemental material for this article is available online.

References

1. DNV. *Floating offshore wind: the next five years*. 2022.
2. Global Wind Energy Council (GWEC). *Offshore wind market report 2022 edition.* 2022.
3. Global Wind Energy Council (GWEC). *Floating offshore wind – a global opportunity. 2022*, 2022.
4. Leimeister M and Kolios A. Reliability-based design optimization of a spar-type floating offshore wind turbine support structure. *Reliab Eng Syst Safety* 2021; 213: 107666.
5. Jiang Z. Installation of offshore wind turbines: a technical review. *Renew Sustain Energy Rev* 2021; 139: 110576.
6. Ramachandran RC, Desmond C, Judge FM, et al. Floating wind turbines: marine operations challenges and opportunities. *Wind Energ Sci* 2022; 7: 903–924. https://doi.org/10.5194/wes-7-903-2022
7. Crowle A and Thies P. Installation innovation for floating offshore wind. Maritime Innovation and Emerging Technologies. Online Conference 2021, 17–18 March 2021.
8. Crowle A and Thies PR. Port and installation constraints of tension leg platforms (TLP) floating wind turbines. In: *Renewable UK/Scottish Renewables. Floating wind 2022 conference, Renewable UK and Scottish Renewables*, Aberdeen, 12 October 2022. pp. 1–28.
9. Amate J, Sánchez GD and González G. Development of a semi-submersible barge for the installation of a TLP floating substructure. TLPWIND ® case study. *J Phys Conf Series* 2016; 749: 012016.
10. Bluewater Energy Services. Large scale floating wind projects: tension leg platforms & the case for offshore in-situ maintenance strategies, 2023. https://floatingwindsolutions.com/wp-content/uploads/2022/03/BramPek_FWS-2022_Bluewater_final.pdf.
11. SBM Offshore SBM offshore launches float4windtm, 2023. https://www.sbmoffshore.com/newsroom/news-events/sbm-offshore-launches-float4windtm
12. Yamada Y, Genovese S, Depew C, et al. Reduce environmental impact and carbon footprint for cost competitive process plant design: integrating AVEVA™ process simulation with modeFRONTIER®. In: Yamashita Y and Kano M (eds) *Computer aided chemical engineering*, Elsevier, Vol. 49, 2022, pp. 211–216. ISSN 1570-7946, ISBN 9780323851596, https://doi.org/10.1016/B978-0-323-85159-6.50035-X.
13. Holtrop J and Mennen G. An approximate power prediction method. *Int Shipbuil Progress* 1982; 29: 168–178.
14. Veritas B. Rules for the classification of steel ships: part B hull and stability, 2024.
15. Papanikolaou A. *Ship design – methodologies of preliminary design*. Berlin/Heidelberg, Germany: Springer, 2014.
16. Klein Woud H and Stapersma D. *Design of propulsion and electric power generation systems*. London: IMarEST Publications, 2002.
17. Sofras E and Prousalidis J. Developing a new methodology for evaluating diesel-electric propulsion. *J Marine Eng Technol* 2014; 13: 63–92.
18. Mrzljak V and Mrakovcic T. Comparison of coges and diesel-electric ship propulsion systems. *J Maritime Transport Sci* 2016; 4: 131–148.
19. Parson MG. Parametric design. In: Lamb T (ed) *Ship design and construction*. Alexandria, VA, USA: Society of Naval Architects and Marine Engineers (SNAME), pp. 11–1 until 11–48, 2003.
20. Kupras LK. Optimisation method and parametric design in precontracted ship design. *Int Shipbuild Prog* 1976; 23: 138–155.
21. Watsom DGM. Practical ship design. *Ocean Eng* 1998; 1: 483–489.

22. Guachamin W, Li L, Gao Z, et al. Methodology for assessment of the operational limits and operability of marine operations. *Ocean Eng* 2016; 125: 308–327.
23. Ship and Bunker. Global port average, 2023. www.shipandbunker.com/prices/av/global/av-g04-global-4-ports-average#MGO.
24. Aalbers A. *Evaluation of ship design alternatives*. Academic Thesis, TU Delft, 2000.
25. Michalski JP. Parametric method of preliminary prediction of the shipbuilding costs. *Polish Marit Res - Spec Issue* 2004; 16–19.
26. Webster I. CPI inflation calculator. 2023. https://www.in2013dollars.com.
27. Hultin D. *Financing sources for shipping - a case study at Wonsild & Son*. MSc thesis, Lund University Department of Business Administration, Sweden. 2004.
28. Pruyn JFJ, van der Burg P, Engelsman A, et al. Ship finance. 2022.
29. Stopford M. *Maritime economics 3E*. 8th ed. New York, NY: Routledge, 2009.
30. Bjerkseter C and Ågotnes A. Floating offshore wind – a global opportunity. 2013.
31. Flierman J. *Innovative installation vessel design for TLP floating wind: exploring the design space by applying a comprehensive modeling approach*. Academic Thesis, TU Delft.